Acta Crystallographica Section B
Structural Science
ISSN 0108-7681

Five more phases of the structural family $[M(H_2O)_2(15\text{-crown-5})](NO_3)_2$

Maxime A. Siegler, Xiang Hao, Sean Parkin and Carolyn Pratt Brock*

Department of Chemistry, University of Kentucky, Lexington, KY 40506-0055, USA

Correspondence e-mail: cpbrock@uky.edu

Received 1 July 2008
Accepted 17 October 2008

The structures of five more phases of the structural family of compounds $[M(H_2O)_2(15\text{-crown-5})](NO_3)_2$ have been determined. All of these phases are stable at room temperature or above, but transform to other phases if cooled slowly. All five phase transitions take place without significant damage to the single crystal. The M = Co phase, which has a three-dimensional hydrogen-bonding pattern, is a disordered version of the structure known at room temperature; Z' changes from 2 to $\frac{1}{2}$. The other four structures have a two-dimensional hydrogen-bonding pattern, are all modulated variants of the same basic cell (or subcell) and are at least mostly ordered. For M = Mg and Zn the structure found somewhat above room temperature is the $Z' = 8$ variant found previously for M = Fe. For M = Cu and Ni the $Z' = 2$ phase found is the same as seen previously for one of the room-temperature polymorphs with M = Mn. There are now two phases and one transition known for each M studied that has a two-dimensional hydrogen-bonding pattern. The changes in the modulation patterns during these transitions are Z' 3 $\leftrightarrow$ 8 (Mg, Fe, Zn), Z' 3 $\leftrightarrow$ 2 (Mn, Ni) and Z' 5 $\leftrightarrow$ 2 (Cu). In all two-dimensional hydrogen-bonded crystals the alternation pattern of conformational enantiomers along the modulation direction becomes more perfect above the phase transition. All stable $[M(H_2O)_2(15\text{-crown-5})](NO_3)_2$ phases whose existence at accessible temperatures is indicated by differential scanning calorimetry (DSC) have now been characterized.

1. Introduction

Ten closely related structures of seven similar compounds $[M(H_2O)_2(15\text{-crown-5})](NO_3)_2$, M = Mg, Mn (three phases), Fe (two phases), Co, Ni, Cu and Zn were determined previously (Hao, Parkin & Brock, 2005; Hao, Siegler *et al.*, 2005; Siegler *et al.*, 2008). All crystals studied (except for those of the Ni compound; see Siegler *et al.*, 2008) were grown at room temperature, although structures were also determined near 90 K. The Co compound and the more stable polymorph[1] of the Mn compound are isostructural; they have a three-dimensional hydrogen-bond pattern (see figures in Hao *et al.*, 2005). The two less stable forms of the Mn compound and the six phases of the other five compounds all have very similar two-dimensional hydrogen-bond patterns (see Fig. 1). The structures of the phases with two-dimensional hydrogen-bonding patterns are all modulated variants ($Z' = 2, 3, 5$ and 8) of a simpler, but disordered, $P2_1/a$, $Z' = \frac{1}{2}$ structure that was

[1] The term polymorph is used here when the two phases are sufficiently different that the transition between them would require nucleation and growth of the new phase. The transition would be expected to either lead to loss of crystallinity or to involve an obvious interface. Modulated variants are different phases (because their diffraction patterns are clearly different) that can be expected to interconvert reversibly and without major crystal damage.

reported for M = Cu at room temperature (Rogers & Song, 1995), but which probably does not exist at that temperature (Hao, Parkin & Brock, 2005). It was shown (Hao, Siegler *et al.*, 2005) that crystals of the two-dimensional hydrogen-bonded phases of the Mn compound and of the Fe compound can be taken through the phase transitions (Z' 3 $\leftrightarrow$ 2 and 3 $\leftrightarrow$ 8, respectively) without any visible loss of crystallinity or any obvious degradation of the diffraction pattern.

We wondered if the $P2_1/a$, $Z' = \frac{1}{2}$ structure reported for M = Cu might be found if the crystals were heated above room temperature. DSC measurements for the Cu compound revealed a reversible phase transition at about 312 K. DSC measurements were therefore made for all the other compounds in the series, and a number of reversible phase transitions just above room temperature were found (see Table 1). As many structures as possible (five) of the newly discovered, higher-temperature phases have been determined. No other structure could be determined, either because the transition was above the limits of the available temperature-control device or because the transition led to decomposition of the crystal.

Table 1
Transition temperatures as determined from endotherms observed in DSC measurements.

Uncertainties in temperatures are at least 2 K.

Metal	First T_{onset} (K)	Other T_{onset} values (K)	Last T_{onset} (K)
Mg	301	353	474
Mn I ($C\bar{1}$)	314	350; 378	418
Mn II ($P4_1$)	329	379	417
Fe	278	(none below 303)	(NA)
Co	306	397	420
Ni	286	(none below 303)	(NA)
Cu	312	370; 382	405
Zn	304	362	421

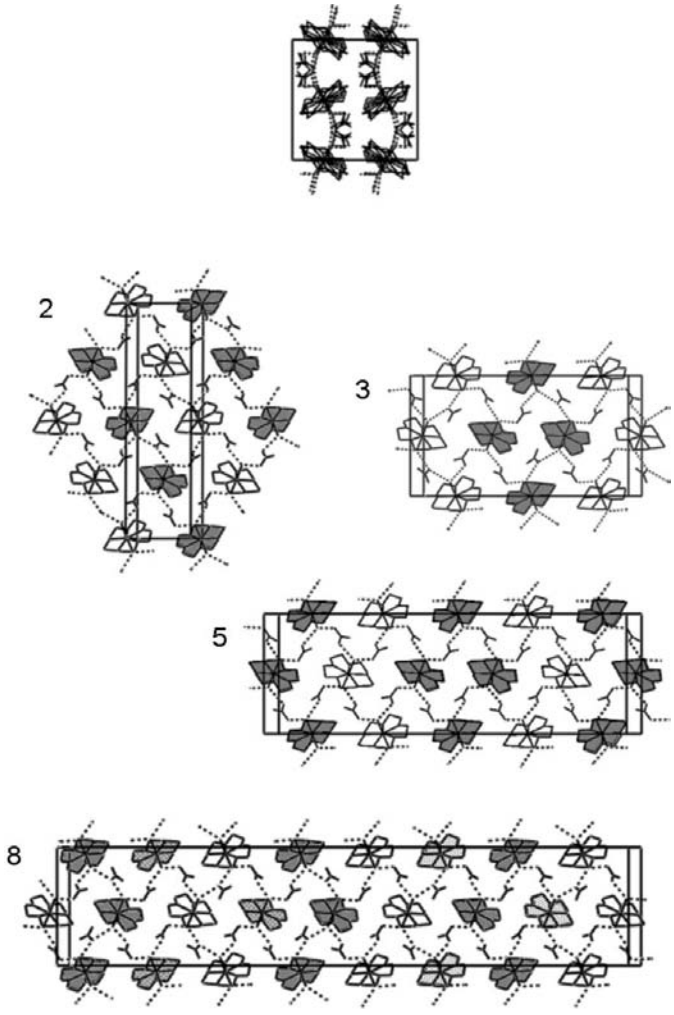

Figure 1
The top drawing shows the projection down the modulation direction (usually **c**) of unit cells of the $[M(H_2O)_2(15\text{-crown-5})](NO_3)_2$ structures with two-dimensional hydrogen-bonding patterns. The other drawings show one layer each of the four different modulated variants, which are labeled by their Z' values. In each case the unit cell is shown. The axial systems for the lower drawings are rotated by 90° around the vertical axis (which is **b**) relative to the top drawing. The horizontal axis for the $Z' = 2$ structure (space group $C\bar{1}$) is [102]; for the other three structures it is **c**. The cations are in contact along the horizontal directions shown but not in the vertical direction. In the lower drawings one of the two sets of conformational enantiomers has been darkened so that the alternation patterns can be seen.

The transitions between ordered phases with two-dimensional hydrogen-bonding patterns are summarized in Fig. 2; the fifth transition, for M = Co, involves a three-dimensional hydrogen-bonding pattern. Crystals can be taken through all transitions shown without any obvious damage. The $P2_1$, $Z' = 8$ structure (reported in the nonstandard group $B2_1$) known previously for M = Fe (Hao, Siegler *et al.*, 2005) is reported here for Mg at 311 K and Zn at 313 K. The $P\bar{1}$, $Z' = 2$ structure (reported in the nonstandard group $C\bar{1}$) known previously for Mn (Hao, Parkin & Brock, 2005) is reported here for Cu at 320 K and Ni at 308 K. The $P4_12_12$, $Z' = \frac{1}{2}$ structure claimed for M = Co at room temperature (Holt *et al.*, 1981; three-dimensional hydrogen-bond pattern) has been determined at 323 K. Some comments about the possible structure of the M = Mn compound above its phase transition at 314 K are also included.

We now know of two, and only two, closely related phases for six of the seven compounds; the seventh, M = Mn, has two polymorphs, with two phases known for one but not for the other. In each case the transitions between the phases involve atom shifts so small that they do not lead to crystal damage.

The divalent metal ions of the two sets of structures in this series (M = Mg, Mn, Fe, Ni, Cu and Zn with two-dimensional hydrogen-bond networks; M = Mn and Co with three-dimensional hydrogen-bond networks) are quite similar, but the different effective ionic radii and the different numbers of d electrons lead to small differences between the cations, *e.g.* in the $M-O_{ether}$ and $M-O_{water}$ bond lengths (see Table 2 of Hao, Siegler *et al.*, 2005). We have not yet been able to identify the structural reasons for the subtle differences between the two- and three-dimensional hydrogen-bond patterns, much less for the differences between the four modulated variants of the two-dimensional hydrogen-bond pattern. We do not know why the Co compound has (so far) been found with only the three-dimensional hydrogen-bond pattern or why five of the

Table 2
Experimental data.

	Fe, $Z' = 8$	Mg, $Z' = 8$	Zn, $Z' = 8$	Ni, $Z' = 2$	Cu, $Z' = 2$	Co, $Z' = \frac{1}{2}$
Crystal data						
Chemical formula	$C_{10}H_{24}O_7Fe^{2+}\cdot 2NO_3^-$	$C_{10}H_{24}O_7Mg^{2+}\cdot 2NO_3^-$	$C_{10}H_{24}O_7Zn^{2+}\cdot 2NO_3^-$	$C_{10}H_{24}O_7Ni^{2+}\cdot 2NO_3^-$	$C_{10}H_{24}CuO_7^{2+}\cdot 2NO_3^-$	$C_{10}H_{24}CoO_7^{2+}\cdot 2NO_3^-$
M_r	436.16	404.62	445.68	439.02	443.85	439.24
Cell setting, space group	Monoclinic, $B2_1$	Monoclinic, $B2_1$	Monoclinic, $B2_1$	Triclinic, $C\bar{1}$	Triclinic, $C\bar{1}$	Tetragonal, $P4_12_12$
Temperature (K)	90.0 (2)	311 (2)	313 (2)	308 (2)	320 (2)	323 (2)
a, b, c (Å)	14.507 (2), 14.226 (2), 68.390 (6)	14.597 (2), 14.135 (2), 70.201 (5)	14.737 (2), 14.050 (2), 69.935 (5)	14.719 (2), 28.041 (3), 10.704 (2)	14.769 (2), 27.924 (3), 10.642 (2)	8.110 (2), 8.110 (2), 27.247 (3)
α, β, γ (°)	90.00, 96.23 (2), 90.00	90.00, 96.95 (2), 90.00	90.00, 96.99 (2), 90.00	90.20 (1), 125.99 (2), 89.870 (1)	89.91 (2), 125.88 (2), 90.06 (2)	90.00, 90.00, 90.00
V (Å^3)	14 031 (3)	14 378 (3)	14 373 (3)	3574.6 (13)	3556.1 (13)	1791.9 (7)
Z	32	32	32	8	8	4
D_x (Mg m^{-3})	1.652	1.495	1.648	1.632	1.658	1.628
Radiation type	Cu $K\alpha$	Cu $K\alpha$	Cu $K\alpha$	Mo $K\alpha$	Mo $K\alpha$	Cu $K\alpha$
μ (mm^{-1})	7.58	1.52	2.56	1.15	1.30	8.17
Crystal form, color	Thick rods, colorless	Block, colorless	Block, colorless	Block, yellow	Block, colorless	Block, purple
Crystal size (mm)	0.30 × 0.15 × 0.11	0.20 × 0.15 × 0.15	0.30 × 0.15 × 0.12	0.35 × 0.15 × 0.15	0.32 × 0.30 × 0.15	0.20 × 0.15 × 0.15
Data collection						
Diffractometer	Bruker–Nonius X8 Proteum	Bruker–Nonius X8 Proteum	Bruker–Nonius X8 Proteum	Nonius KappaCCD	Nonius KappaCCD	Bruker–Nonius X8 Proteum
Data collection method	ω and φ scans	ω and φ scans	ω and φ scans	ω scans at fixed χ = 55°	ω scans at fixed χ = 55°	ω and φ scans
Absorption correction	Multi-scan†	Multi-scan†	Multi-scan†	Multi-scan†	Multi-scan†	Multi-scan†
T_{min}	0.20	0.751	0.514	0.688	0.681	0.193
T_{max}	0.47	0.804	0.749	0.846	0.829	0.292
No. of measured, independent and observed reflections	89 101, 25 223, 15 621	53 583, 22 712, 10 777	91 322, 25 529, 12 218	12 132, 6301, 4268	15 229, 8078, 6313	21 414, 1635, 1509
Criterion for observed reflections	$I > 2\sigma(I)$	$I > 2\sigma(I)$	$I > 2\sigma(I)$	$I > 2\sigma(I)$	$I > 2\sigma(I)$	$I > 2\sigma(I)$
R_{int}	0.050	0.030	0.046	0.037	0.023	0.063
θ_{max} (°)	68.2	65.5	68.3	25.0	27.5	68.2
Refinement						
Refinement on	F^2	F^2	F^2	F^2	F^2	F^2
$R[F^2 > 2\sigma(F^2)]$, $wR(F^2)$, S	0.043, 0.125, 1.13	0.058, 0.181, 1.51	0.055, 0.189, 1.46	0.045, 0.125, 1.05	0.037, 0.099, 1.11	0.041, 0.109, 1.28
No. of reflections	25 223	22 712	25 529	6301	8078	1635
No. of parameters	892	892	892	494	494	170
H-atom treatment	Mixture‡	Mixture‡	Mixture‡	Mixture‡	Mixture‡	Mixture‡
Weighting scheme	$w = 1/[\sigma^2(F_o^2) + (0.050P)^2]$, where $P = (F_o^2 + 2F_c^2)/3$	$w = 1/[\sigma^2(F_o^2) + (0.050P)^2]$, where $P = (F_o^2 + 2F_c^2)/3$	$w = 1/[\sigma^2(F_o^2) + (0.050P)^2]$, where $P = (F_o^2 + 2F_c^2)/3$	$w = 1/[\sigma^2(F_o^2) + (0.064P)^2]$, where $P = (F_o^2 + 2F_c^2)/3$	$w = 1/[\sigma^2(F_o^2) + (0.050P)^2]$, where $P = (F_o^2 + 2F_c^2)/3$	$w = 1/[\sigma^2(F_o^2) + (0.070P)^2]$, where $P = (F_o^2 + 2F_c^2)/3$
$(\Delta/\sigma)_{max}$	0.002	0.002	0.002	0.001	0.002	< 0.0001
$\Delta\rho_{max}$, $\Delta\rho_{min}$ (e Å^{-3})	0.77, −0.43	0.48, −0.35	0.64, −0.46	0.65, −0.52	0.44, −0.41	0.34, −0.24
Extinction method	*SHELXL*	*SHELXL*	*SHELXL*	None	None	*SHELXL*
Extinction coefficient	0.000058 (3)	0.000071 (5)	0.000049 (3)	–	–	0.0084 (9)
Absolute structure	–	–	–	–	–	Flack (1983)
Flack parameter	–	–	–	–	–	−0.007 (7)

Computer programs used: *APEX*2 (Bruker–Nonius, 2004), *COLLECT* (Nonius, 1999), *SAINTPlus* in *APEX*2 (Bruker–Nonius, 2004), *SCALEPACK* (Otwinowski & Minor, 2006), *DENZO-SMN* (Otwinowski & Minor, 2006), *SHELXS*97, *SHELXL*97 (Sheldrick, 2008), *MERCURY* (Macrae *et al.*, 2006), local procedures. † Based on symmetry-related measurements. ‡ Mixture of independent and constrained refinement.

six other compounds seem to crystallize with only a two-dimensional hydrogen-bond network. Nor do we understand what feature of the Mn compound leads to its being found in both polymorphs. We do not understand why the low-temperature phase of the Cu compound has $Z' = 5$ when the low-temperature phases for the other five compounds with two-dimensional hydrogen-bonding have $Z' = 3$.

We also report a sixth structure: the redetermination at 90.0 (2) K, with more intense data, of the $P2_1$, $Z' = 8$ structure of the Fe compound (Hao, Siegler *et al.*, 2005). The Fe compound, which forms at room temperature as the $Z' = 8$ phase but transforms to the $Z' = 3$ phase at *ca* 278 K if cooled slowly (2 K min^{-1}), is the only one of the known high-temperature phases that can be retained at 90 K as metastable

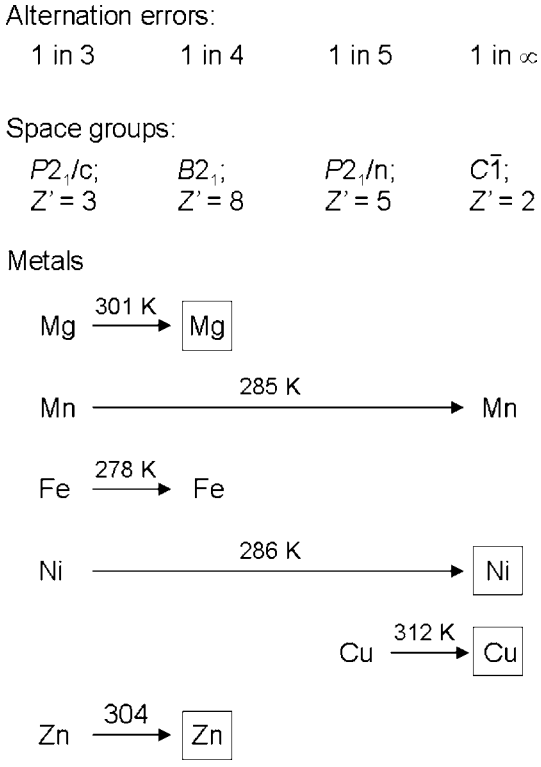

Figure 2
Diagram showing the known two-dimensional hydrogen-bonded phases for $[M(H_2O)_2(15\text{-crown-5})](NO_3)_2$ compounds. The transition temperatures between the two phases known for each compound are also shown. The four boxes indicate the new structures reported in this paper. All other structures shown were reported previously (Hao, Parkin & Brock, 2005; Hao, Siegler *et al.*, 2005; Siegler *et al.*, 2008).

if flash cooled. It is our experience that the other high-temperature phases with a two-dimensional hydrogen-bond pattern all transform to the $Z' = 3$ phase (M = Mg, Ni, Zn) or $Z' = 5$ phase (Cu) even if cooled as quickly as possible[2] to 90 K from a temperature at the lower end of the stability range of the phase. The high-temperature M = Co structure, which has a three-dimensional hydrogen-bond pattern, also transforms easily and reversibly to the form stable at lower temperatures.

2. Experimental

2.1. DSC studies

Crystals of the Mg, Co, Cu and Zn compounds, and of both the triclinic and tetragonal phases of the Mn compound, were prepared as described earlier (Hao, Parkin & Brock, 2005; Hao, Siegler *et al.*, 2005), washed with water and acetone, and dried under vacuum. The resulting crystals of each compound were ground into fine powders. A small amount (5–20 mg) of each sample was sealed in an aluminum pan. All measurements for these five compounds were performed on a 2920 Modulated DSC apparatus from TA Instruments operating between room temperature and *ca* 440 K. The heating rate was 1 K min^{-1} for $T < 333$ K, and 5 K min^{-1} for $T > 333$ K. Two samples of each compound were studied. Files showing the DSC traces for M = Mg, Mn (both polymorphs), Co, Cu and Zn are given in Appendix C of Xiang Hao's dissertation (2005), which is available electronically at http://lib.uky.edu/ETD/ukychem2005d00317/XHaoDiss.pdf. The traces have also been deposited with the supplementary material for this paper.[3]

The thermal behaviors of the Fe (Hao, Siegler *et al.*, 2005) and Ni compounds (Siegler *et al.*, 2008) were investigated using a DSC 822 apparatus and the controlling software *STARe* (Version 8.10) manufactured by METTLER TOLEDO. This instrument can make measurements below room temperature, which the other instrument cannot; scans were made between 250 and 303 K using heating rates of 5, 10 and 20 K min^{-1}. All samples contained about 2.0 mg of a fine powder. Two of the DSC traces for M = Fe and Ni are given in Chapters 2 and 3 of Maxime A. Siegler's dissertation (2007), which is available electronically at http://lib.uky.edu/ETD/ukychem2007d00664/dissertationMASiegler.pdf. These traces have also been deposited with the supplementary material for this paper.

A list of the transition temperatures (T_{onset}) observed is given in Table 1; the last transition temperature probably corresponds to decomposition rather than melting (ΔH° *ca* 50 kJ mol^{-1}). The onset temperatures were determined using the instrument software and depend to some extent on sample history and scan rate; uncertainties are at least 2 K. In most cases the temperature given is the average of T_{onset} for heating and cooling runs. Most of the $\Delta_{tr}H^\circ$ values are so small that they could be determined only very approximately; the values were mostly in the range 0.1–1 kJ mol^{-1}. For the phases that are tetragonal at room temperature (Co compound and the more stable of the two Mn phases) the ΔH° value for the penultimate transition is about 10 kJ mol^{-1}.

2.2. Structure determinations

All previously unknown phases indicated by the DSC traces as having T_{tr} below 320 K were studied by single-crystal X-ray diffraction. It was, however, impossible to study the transition of the tetragonal Mn phase, which takes place at 329 K (see Table 1) because of limitations of the temperature-control device available.

Most structures were determined 9–14 K above T_{tr} to insure that the transition was complete. The Co phase was studied 17 K above its T_{tr} and the Ni phase 22 K above its T_{tr}. Data for the monoclinic Mn phase were collected only 7 K above the transition (*i.e.* at 321 K), but even at that temperature

[2] During flash cooling a crystal at room temperature is placed in an N_2(g) stream already at $T = 90$ K; the temperature of the crystal drops very rapidly. The cooling rate for a crystal that is already on the diffractometer at or above room temperature is much slower because the rate of cooling is limited by the design of the temperature controller, which cannot lower the temperature of the gas stream from 293 to 90 K in less than several minutes. We did not attempt to develop any special techniques for very rapid cooling.

[3] Supplementary data for this paper are available from the IUCr electronic archives (Reference: BS5069). Services for accessing these data are described at the back of the journal.

decomposition made detailed structure determination impossible.

Single crystals of the Mg, Mn, Fe, Co, Cu and Zn compounds were grown as described previously (Hao, Parkin & Brock, 2005; Hao, Siegler *et al.*, 2005). Crystals of the Ni compound were prepared by a more complicated route (Siegler *et al.*, 2008). Crystals of the Fe compound that are grown at room temperature are in the $Z' = 8$ phase, and remain in that phase when flash-cooled to 90 K. Crystals of the Ni compound, which must be grown at elevated temperatures (Siegler *et al.*, 2008) and then cooled are in the high-temperature $Z' = 2$ phase at room temperature. Crystals of the other four compounds were grown at room temperature and then warmed through a phase transition while mounted on the diffractometer.

Two diffractometers were used; both were equipped with the same CryoCool LN2 temperature-control system (Cryo Industries of America, Manchester, NH). Data for the two triclinic, $Z' = 2$ structures (Cu and Ni), both of which are ordered, and for the Mn crystal that decomposed, were measured with a Nonius KappaCCD diffractometer with Mo $K\alpha$ radiation from a sealed tube. Data for the Co structure (very disordered) and for the Mg, Zn and Fe structures (modulated superstructures with $Z' = 8$ and many systematically weak reflections) were measured with a Bruker–Nonius X8 Proteum diffractometer using Cu $K\alpha$ radiation. The greater than 10^3-fold increase in recordable diffracted X-rays in going from a sealed-tube Mo $K\alpha$ source to a rotating-anode source with Bruker Helios graded multilayer focusing optics more than offset the increase in absorption, which was very significant for Fe and Co (increases in μ by factors of 8.2 and 8.3).

In all cases the data in the frames were transformed to show reconstructed slices $nk\ell$, $hn\ell$ and hkn, n = 0–3, of the reciprocal lattice. Careful examinations of these slices showed that the crystals (except for the Mn phase studied at 321 K) were phase pure.

During the final refinements the H atoms of the 15-crown-5 ligands were placed at calculated positions [instruction AFIX 23 in *SHELXL*97 (Sheldrick, 2008)] with isotropic displacement parameters having values $1.2U_{eq}$ of the attached C atom. The H atoms of water ligands for the ordered structures were located in difference-Fourier maps and restrained such that the O—H distances and H—O—H angles had values within accepted ranges [d(O—H) = 0.82–0.84 Å, d(H···H) $\simeq$ 1.30 Å so that H—O—H $\simeq$ 104.5°]. For the water H atoms U_{iso} = $1.5U_{eq}$ of the attached O atom. The atom-numbering schemes were made consistent with those of previously published structures having the same phase type (*i.e.* the same Z'). The basic numbering system for the crown ligand is shown in Fig. 3; atoms O6 and O7 belong to the axial water ligands. For the structures with $Z' > 2$ the residue numbering system available in *SHELXL*97 (Sheldrick, 2008) was very useful.

Information about the structure determinations can be found in Table 2 and the supplementary material. The estimated errors in the unit-cell constants were obtained by multiplying the values given by the software by at least a factor of 3 for the cell constants and by at least a factor of 15 for the cell angles. These factors were used in order to take into account the variations in the unit-cell constants from one crystal to another (Herbstein, 2000). Some additional details are given below.

2.2.1. $B2_1$, $Z' = 8$ structures (Fe, Mg, Zn). The structure of the Fe compound has been reported previously (Hao, Siegler *et al.*, 2005) for crystals grown at room temperature and flash-cooled to 90 K, where they are metastable. In that structure determination, which used data from the KappaCCD diffractometer described above, 52% of the reflections to $(\sin\theta/\lambda)_{max}$ = 0.60 Å^{-1} had $I > 2\sigma(I)$, while for the data reported here from the Proteum diffractometer 62% of the reflections had $I > 2\sigma(I)$ for the same range. Improvements in the intensity measurements for the weakest subset of reflections, those with $\ell = 8n + 4$, were especially significant. Because data for the corresponding Mg and Zn structures had to be collected above room temperature the fractions of reflections having $I > 2\sigma$ were very low for those two structures. For the Zn structure the percentage of 'observed' reflections (see Table 2) to $\sin(\theta/\lambda)$ = 0.60 Å^{-1} was 48% when data were collected with the Proteum diffractometer, but only 27% when data were collected under similar conditions on the KappaCCD diffractometer. The corresponding percentages for the Mg compound would have been even more disparate.

No special problems were encountered in indexing the frames or processing the data for these three structures. The **c** axis for each is very long, but the cell is centered so that half of the reflections $hk\ell$ are absent. The crystal-to-detector distance was 60 mm for the Mg compound and 42 mm for the Fe and Zn compounds. The reciprocal-lattice slices reconstructed from the minimally processed (or 'raw') frames were examined especially carefully but no unusual feature was found. All reflections occur right at their predicted positions and all

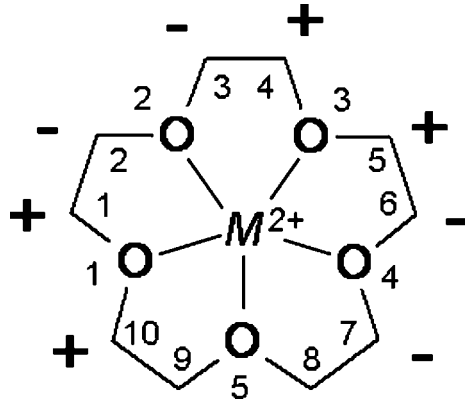

Figure 3
Line drawing of the 15-crown-5 ligand as it is found coordinated to the metal ions in the structures $[M(H_2O)_2(15\text{-crown-}5)](NO_3)_2$. The five O atoms and the metal ion are approximately coplanar; the plus and minus signs indicate the deviations of the C atoms from that plane. The deviations of the two C atoms at the bottom of the drawing are much smaller than for the other eight because the pattern cannot be closed around a 15-crown 5 ring. The two conformational enantiomers of these cations differ in the signs of the deviations of the C atoms from the approximate plane.

reflections had similar spot shapes. We found no indication that the modulation might be incommensurate.

The $P2_1$ unit cells determined by the diffractometer software were transformed to the nonstandard $B2_1$ setting so that the modulation would be along [001] rather than along [102]. The $B2_1$ cell is easier to compare with the cells for the other phases. The cell transformation is $\mathbf{a}(B2_1) = (100/0\bar{1}0/\bar{1}0\bar{2})\,\mathbf{a}(P2_1)$.

Separate Wilson plots (Xia *et al.*, 2001, 2002) for the $\ell = 8n$, $8n \pm 1$, $84n \pm 2$, $8n \pm 3$ and $8n \pm 4$ classes of reflections for the Fe structure (data at 90 K) and the Zn and Mg structures (data at 313 and 311 K) are shown in Figs. 4 and 5. Above room temperature the $8n \pm 4$ reflections for the Mg and Zn phases are so weak that the average value is sometimes slightly negative; for these reflections the calculated (open circles) rather than observed values (filled circles) are shown. The intensities of the $\ell = 8n \pm 4$ reflections measured for the Fe phase at 90 K are much more reliable, as is shown by the relatively smooth curve at the bottom of Fig. 4. For the Fe structure at 90 K the average intensity of the $\ell = 8n \pm 4$ reflections (and of the $\ell = 8n \pm 2$ reflections) rises with $(\sin\theta/\lambda)^2$ because the decrease in average intensity with scattering angle that results from thermal motion and disorder is less important than the increase in intensity that results from the increasing resolution. The increase in intensity with $(\sin\theta/\lambda)^2$ of the Fe $\ell = 8n \pm 4$ reflections demonstrates that these reflections are not systematically absent.

There is enantiomeric disorder at two of the eight cation sites (residues 3 and 7) in all three structures. Occupancy factors for the two sites were refined independently but are indistinguishable or nearly so (0.893 and 0.878 for Fe at 90 K; 0.732 and 0.737 for Mg at 311 K; 0.738 and 0.735 for Zn at 313 K; all s.u.s 0.002). All three structures were found to be racemic. Twin fractions refined to 0.503 (6), 0.62 (10) and 0.55 (8) for the Fe, Mg and Zn structures, and so were all set to 0.50 in the final cycles.

The Fe structure at 90 K could be refined with only a few geometrical restraints. One restraint was needed to fix the origin. Two others were imposed to set target values of the O—H and H···H distances in the water ligands to 0.82 (1) and 1.30 (2) Å; these two distances together should lead to an H—O—H angle of *ca* 104.9°. Rigid groups were used to describe the minor components at the two sites of cation disorder. Eighteen sets of EADP instructions were used to make the displacement ellipsoids for corresponding atoms of the eight cations identical; eight more sets of EADP instructions were used for the four atoms in the two groups of nitrate anions. Constraining the ellipsoids in this way is reasonable because all corresponding atoms are related by either pseudotranslation or pseudoinversion. There was no problem with conver-

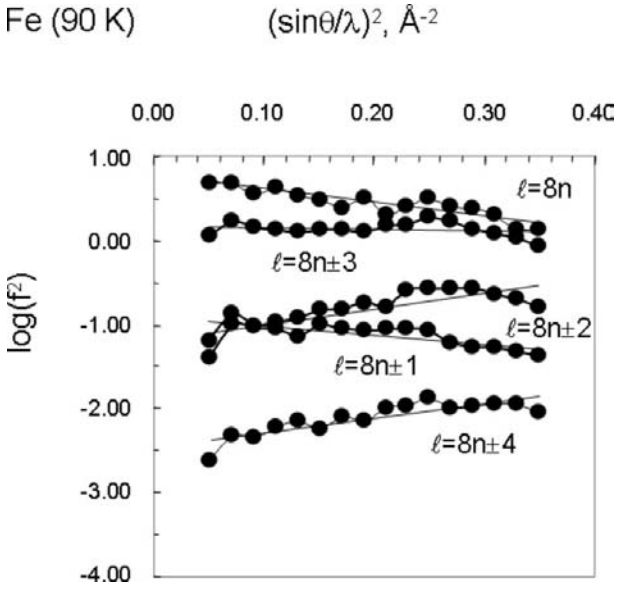

Figure 4
Separate Wilson plots for the 00ℓ, $\ell = 8n \pm m$ reflections measured at 90 K for the $Z' = 8$ phase of the Fe compound. The origin of the vertical scale is arbitrary.

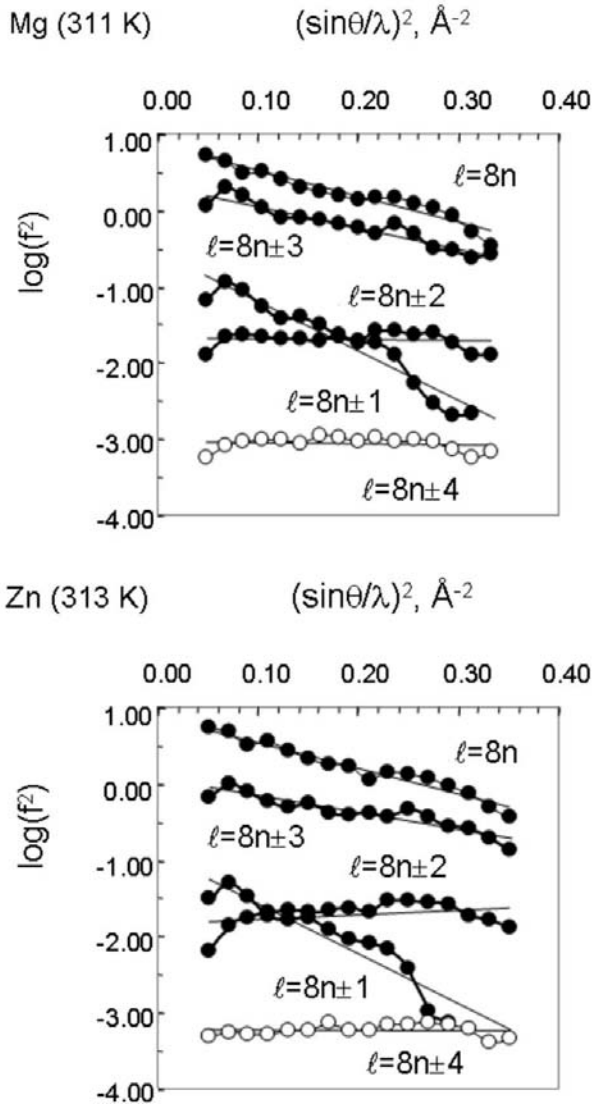

Figure 5
Separate Wilson plots for the 00ℓ, $\ell = 8n \pm m$ reflections measured at 311 K for the $Z' = 8$ phase of the Mg compound, and at 313 K for the $Z' = 8$ phase of the Zn compound. The open circles correspond to calculated values (see text). The origin of the vertical scale is arbitrary.

gence. There were no unusual bond lengths or angles such as might result from correlation problems.

The Mg and Zn structures (311 and 313 K) could not be refined successfully without additional geometrical constraints. The minor components at the two sites of cation disorder were refined as rigid groups. The SAME instruction was used, with an effective standard uncertainty of 0.025 Å, to keep corresponding bonded and 1,3 distances (and therefore corresponding bond angles) similar for all the other cations and for all the anions. The H atoms of the water ligands were restrained as described above. The displacement ellipsoids for these two structures are shown in Fig. 6, which also shows the ellipsoids for the Fe structure and the atom-numbering scheme.[4]

Convergence of the Mg and Zn refinements was very slow, probably because there were correlation coefficients of *ca* ±0.9 involving the water H atoms. There is a large peak (0.76 e Å^{-3}) near one of the O atoms of a nitrate ion in the Fe structure (O8_26, which is hydrogen-bonded to O6_8). The major peaks and troughs are otherwise approximately equal in size, but the major peaks are mostly associated with the O atoms of nitrate ions. The motions of the nitrate ions around their approximate threefold axes may be large enough above 300 K that the harmonic approximation is inadequate.

2.2.2. $C\bar{1}$, Z' = 2 structures (Ni, Cu). The Ni and Cu structures (at 308 and 320 K, respectively) are isostructural with that of Mn crystals grown at room temperature (Hao, Siegler *et al.*, 2005); the atom-numbering systems in the three structures are the same. The nonstandard space group $C\bar{1}$ was chosen as it was for the Mn structure; this nonstandard setting was chosen to facilitate comparisons with other structures in the series. Crystals were pseudomerohedrally twinned by a 180° rotation around **b** [twin fractions 0.691 (2) and 0.418 (2) for the Ni and Cu crystals]. Structure refinements were otherwise straightforward.

In the Ni structure the displacement ellipsoids for the Ni ions and water O atoms are somewhat elongated in the general direction of the coordinated atoms O1 and O4 (see Fig. 7 or a view of the ellipsoids generated from the data in the CIF). In the structure of the $P2_1/c$, Z' = 3 phase (Siegler *et al.*, 2008) a disorder of the Ni ion can be resolved at 90 K; the split Ni-ion position is probably a consequence of the small size of the Ni^{2+} ion (Greenwood & Earnshaw, 1997) and its preference for octahedral coordination (see Siegler *et al.*, 2008). We believe the elongations of the Ni ellipsoids in the triclinic structure occur for the same reason. Those elongations, however, were by no means large enough to justify the use of a split-atom disorder model.

2.2.3. Mn I phase at 321 K. This phase was produced by heating a monoclinic Z' = 3 crystal with a two-dimensional hydrogen-bonding pattern. Data were collected just 7 K above the transition temperature measured by DSC, but the crystal decomposed rapidly over the 2–3 h of data collection. We could see through the microscope that parts of the crystal became dark, which suggested it had become partially polycrystalline and had perhaps lost water. Data collection had to be terminated prematurely (fraction complete to 0.60 Å^{-1} = 0.88) because of degradation of the peak shape.

We had thought that this phase might be the $P2_1/c$, $Z' = \frac{1}{2}$ phase first proposed for M = Cu by Rogers & Song (1995). The instrument software did find a unit cell with the expected dimensions, but careful examination of the reconstructed reciprocal lattice (or RL) slices showed that cell to be only an approximation. Many of the spots in the RL slices were very large. Others were very small and close together in the **c*** direction. Parts of powder rings could be seen. Twinning is a possibility, as is the presence of more than one phase. A transition to a phase with a higher Z' value cannot be ruled out. We concluded, with considerable regret, that we would be unable to determine the details of the structure of the Mn

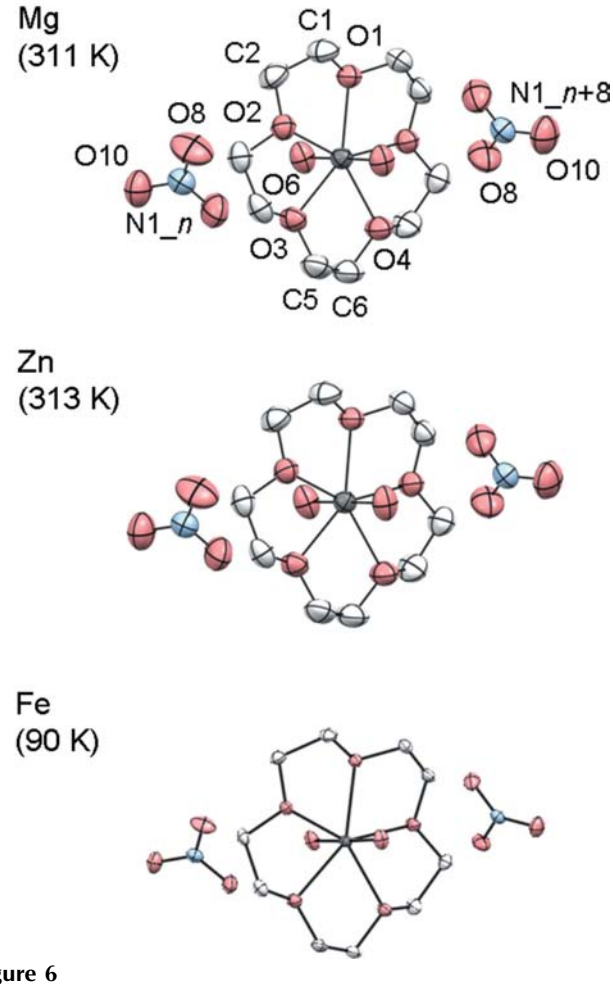

Figure 6
Perspective drawings of a typical formula unit of the Z' = 8 phase of the Mg compound at 311 K, the Zn compound at 313 K, and the Fe compound at 90 K. Ellipsoids are drawn at the 50% probability level and H atoms have been omitted in this and all subsequent drawings. The displacement ellipsoids for corresponding atoms are the same (see text) for all eight ion pairs in the asymmetric unit of each compound. Information about the atom-numbering scheme, which is the same for all compounds, is shown in the top drawing. Atom numbers not shown can be worked out from the scheme described in the text.

[4] The residue-numbering option available in *SHELXL*97 (Sheldrick, 2008) was very useful. Residues _1 through _10 are the eight independent cations, two of which are disordered. Residues _11 through _26 are the 16 independent nitrate ions.

crystal with a two-dimensional hydrogen-bond pattern above its phase transition at 314 K. We can say, however, that the major phase present has the same subcell as all the other $[M(H_2O)_2(15\text{-crown-}5)](NO_3)_2$ two-dimensional hydrogen-bonded structures in the series.

2.2.4. $P4_12_12$, $Z' = \frac{1}{2}$ structure (Co). This structure was reported by Holt *et al.* (1981) at room temperature, but we believe the room-temperature structure to be in the space group $P4_1$ with $Z' = 2$ (Hao, Siegler *et al.*, 2005). At 320 K it was necessary to collect data using the rotating-anode Cu $K\alpha$ source, even though the absorption was large, to be sure that the reflections indicative of the larger $P4_1$ cell had actually disappeared completely and because the extensive disorder and high thermal motion caused all reflections to be weak. The cation is located on a twofold axis parallel to [110], which nearly superimposes pairs of C atoms (see Fig. 8). Constraints that used 24 of the 'free variables' available in *SHELXL*97 were imposed on the U^{ij} values for these pairs of atoms (C1/C7, C2/C6, C3/C5, C8/C10) so that the two ellipsoids in each pair would be the same even though the two have different orientations. The Co ion had to be constrained to lie on the twofold axis because if it were not the refinement became unstable. Restraints on the crown ligand C—O and C—C bond lengths proved necessary; the target values [1.430 (5) and 1.496 (5) Å] were the average values determined for the structure with M = Mg at 294 K ($P2_1/c$, $Z' = 3$). If these restraints were not imposed the bond lengths became unacceptably short. Convergence was slow, probably because of large (±0.80 and beyond) correlation coefficients. This structure has not been, and probably cannot be, determined very precisely.

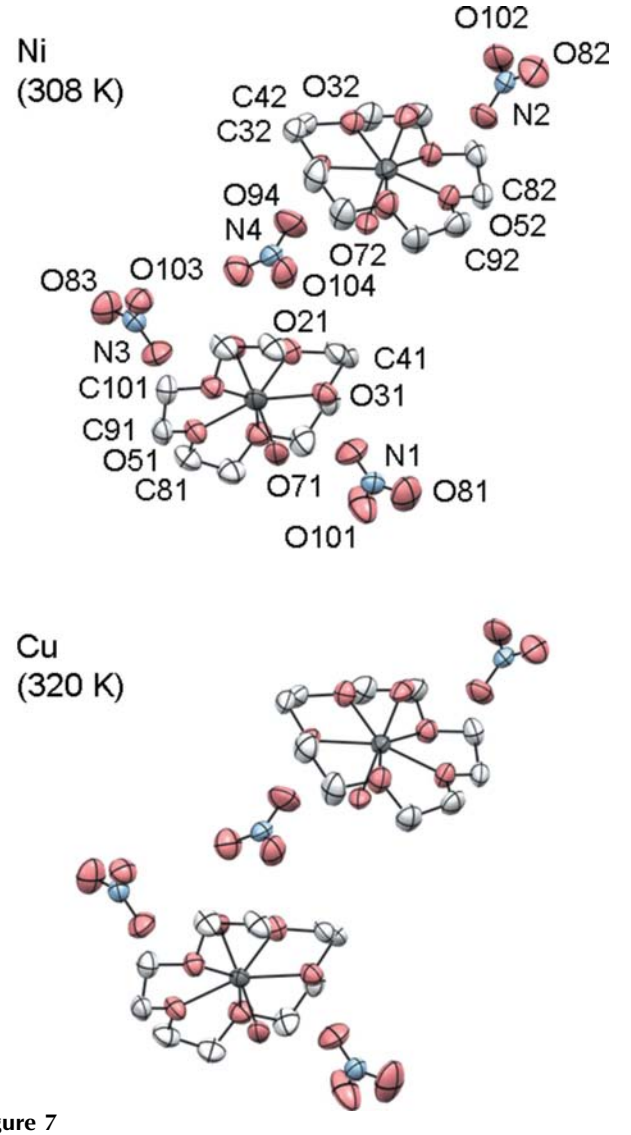

Figure 7
Perspective drawings of the asymmetric units of the $Z' = 2$ phase of the Ni compound at 308 K (upper drawing) and the Cu compound at 320 K (lower drawing). Ellipsoids are drawn at the 50% probability level. Information about the atom numbering scheme, which is the same for both compounds, is shown in the upper drawing. Atom numbers not shown can be worked out from the scheme described in the text.

3. Results

3.1. Phase transitions

Each of the seven compounds $[M(H_2O)_2(15\text{-crown-}5)](NO_3)_2$, M = Mg, Mn, Fe, Co, Ni, Cu and Zn, has a reversible phase transition just above room temperature (Mg, Co, Cu, Zn) or just below room temperature [Mn (polymorph I), Fe, Ni; see Table 1 and Fig. 2] after which the crystal continues to have a high-quality diffraction pattern that can be indexed with a single axial system. The Mn I compound (two-dimensional hydrogen-bond pattern) has a second phase transition at 314 K, but the transition leads to so much crystal damage that the details of the structure could not be determined.

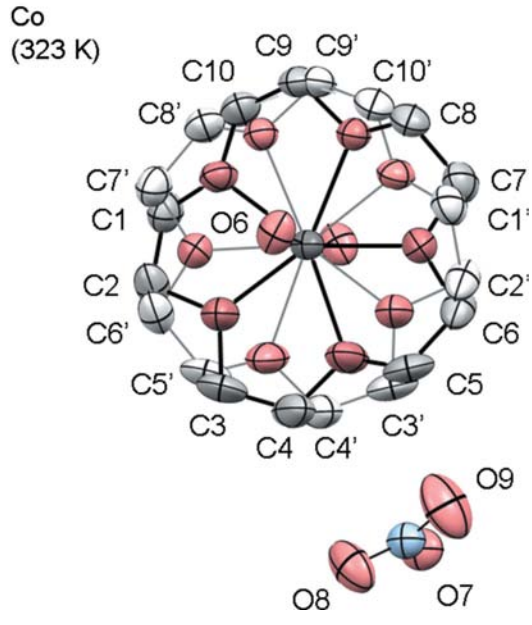

Figure 8
Perspective drawing of the asymmetric unit of the $Z' = \frac{1}{2}$ phase of the Co compound at 323 K. The cation lies on an inversion center and is therefore disordered. Ellipsoids are drawn at the 50% probability level. Information about the atom numbering scheme is shown. Atom numbers not shown can be worked out from the scheme described in the text.

For the Co compound (three-dimensional hydrogen-bond pattern) the transition seems to be a simple order–disorder transition during which the cations become disordered around twofold axes.

For the six compounds having two-dimensional hydrogen-bond patterns the transition involves a change in the alternation pattern of the conformational enantiomers of the 15-crown-5 ligand (see Figs. 3 and 10 of Hao, Parkin & Brock, 2005). This alternation is along the **c** axis in the monoclinic structures and along [102] in the triclinic structures. Four different types of alternation pattern have been seen (see Fig. 2). Three types of transitions have been found: changes in Z' of 3 $\leftrightarrow$ 8 (Mg, Fe, Zn), 3 $\leftrightarrow$ 2 (Mn, Ni) and 5 $\leftrightarrow$ 2 (Cu). The changes in atomic positions necessary to change the alternation pattern are large enough that they lead to obvious changes in the diffraction pattern, but not so large as to cause significant damage to the macroscopic crystal. The largest components of the atomic motions lie within the best planes of the crown ligands.

3.2. Descriptions of modulations in the layered structures

The Z' = 2, 3, 5 and 8 structures are all modulated variants of the same basic structure, which was reported (Rogers & Song, 1995), but which probably does not exist for Cu below at least 320 K (Hao, Parkin & Brock, 2005; Hao, Siegler *et al.*, 2005; this work) and may not exist at all. The monoclinic structures all have hydrogen-bonded layers that extend in directions perpendicular to **a*** (*i.e.* along **b** and **c**); the corresponding normal direction in the triclinic crystals is $(20\bar{1})$. Within a layer the cations and anions are connected by hydrogen bonds. There are no strong attractions between layers, which are separated by $a/2$ in the monoclinic structures (see Fig. 1).

In the basic structure (space group $P2_1/c$ with $Z' = \frac{1}{2}$) cations would be located at inversion centers and would therefore be disordered. In the modulated structures the **a** axis is doubled, and cations adjacent along **a** are conformational enantiomers. If cations adjacent along **a** were not related by inversion there would be short, unfavorable contacts between them. The **c** axis in the modulated structures is also lengthened; the approximate multipliers are the Z' values. Along **c** there is a pattern of alternation of conformational enantiomers such that in the Z' = 3 structure a row of cations has the pattern ..., R, R, S, R, R, S, ... or ..., S, S, R, S, S, R, ..., which means that the conformational enantiomers fail to alternate at every third opportunity. For the Z' = 5 structure the enantiomers fail to alternate every fifth opportunity, and for the Z' = 8 (*B*-centered) structure the alternation fails two times in eight, or one in four. In the triclinic structure the alternation is perfect. The two other obvious possibilities, which have not been seen, are failure to alternate every second opportunity, which would give the pattern ..., R, R, S, S, R, R, S, S, ..., or complete failure to alternate, which would give homochiral rows.

We believe these modulations to be commensurate, or at least nearly so (see below). The agreement between predicted and observed reflection positions and the relatively large fraction of superstructure reflections with measurable intensities both point to a commensurate modulation. Furthermore, many of the structures in this series, including the M = Cu structure with Z' = 5 and the M' = Fe structure with Z' = 8 have been studied both at room temperature and at 90 K (the M = Fe structure being flash-cooled to prevent transition to the Z' = 3 phase). The cells at those very different temperatures are always the same if allowance is made for thermal contraction.

3.3. Alternate cell choice for the triclinic structure

We originally reported the triclinic M = Mn structure (Hao, Siegler *et al.*, 2005) in the non-standard space group $C\bar{1}$ rather than the standard group $P\bar{1}$ because in the former the layer includes the **b** axis, while in the latter the hydrogen-bonded layer is described by $(11\bar{1})$. The transformation to the non-standard cell is given by $\mathbf{a}_C = (\bar{1}\bar{1}0/\bar{1}\bar{1}\bar{2}/100)\,\mathbf{a}_P$. The M = Ni and Cu structures reported in this paper are described in the same space group for consistency, but we now realise it would have been better to use the non-standard group $F\bar{1}$, where $\mathbf{a}_F = (\bar{1}\bar{1}0/112/\bar{1}10)\,\mathbf{a}_P = (100/0\bar{1}0/\bar{1}0\bar{2})\,\mathbf{a}_C$.

In the $F\bar{1}$ description the hydrogen-bonded layers include the **b** and **c** axes, as they do in the other three structure types seen in this series. The angles α and γ are very close to 90° (see Table 3) so the cell is seen to be pseudo-monoclinic. For the Z' = 3, 5 and 8 structures the axial lengths are $2a_{\rm basic}$, $b_{\rm basic}$ and $Z'c_{\rm basic}$, where the basic cell (or subcell) is that described by Rogers & Song (1995) for the supposed $Z' = \frac{1}{2}$ structure, and the β angle is in the range 96–97°. The axial lengths for the $F\bar{1}$ cell are $2a_{\rm basic}$, $2b_{\rm basic}$ and $Z'c_{\rm basic}$, where Z' = 2. The β angle is in the range 96–98°. The important difference between the triclinic Z' = 2 structure and the monoclinic Z' = 3, 5 and 8 structures is the doubling of the **b** axis in the triclinic, Z' = 2 structure.

3.4. Symmetry relationships among the phases

In the $P2_1/c$, $Z' = \frac{1}{2}$ subcell all cations are disordered over inversion centers. Adjacent hydrogen-bonded layers that contain **b** and **c** axes are related by the translation along **a**, by inversion, and by a 2_1 screw operation. The $P2_1/c$, Z' = 3 cell is the low-temperature form for five of the six compounds with a two-dimensional hydrogen-bonding pattern. In that cell adjacent hydrogen-bonded layers are still related by $\bar{1}$ and 2_1 operations, but the number of such symmetry elements per formula unit is reduced by three relative to the subcell. The glide planes relate ions in the same hydrogen-bonded layer. In the Cu compound ($P2_1/n$, Z' = 5) the number of $\bar{1}$ and 2_1 operations is reduced by five relative to the subcell and the effects of the glide planes and 2_1 axes is reversed relative to the Z' = 3 structures: adjacent layers in the Z' = 5 structure are related by inversion centers and n glide planes, while ions within layers are related by the 2_1 axes. In the high-temperature $P2_1$, Z' = 8 cell there are 2_1 axes within the hydrogen-bonded layers and between them but no inversion centers or glide planes. Layers are also related by the centering operation. In the triclinic, Z' = 2 cells all the 2_1 axes and glide planes have been lost, but there are inversion centers between and

Table 3
Cell constants for the triclinic structures ($Z' = 2$) referred to an *F*-centered cell (see text).

	M = Mn[a]	M = Ni	M = Cu
T (K)	294	308	320
a (Å)	14.730	14.719	14.769
b (Å)	28.329	28.041	27.924
c (Å)	17.559	17.453	17.397
α (°)	89.98	90.14	89.94
β (°)	96.66	97.04	97.58
γ (°)	89.95	90.13	89.94

References: (*a*) Hao, Siegler *et al.* (2005).

within the hydrogen-bonded layers. Within the hydrogen-bonded layers there are inversion centers in, but not between the hydrogen-bonded rows along $[102]_C = [001]_F$ (see Fig. 1).

4. Discussion

4.1. Order of the phase transitions

It seems likely that the transitions in the crystals with two-dimensional hydrogen-bond patterns are all first order because the changes in symmetry are significant and because both structures are at least mostly ordered. For M = Ni the width of the hysteresis loop associated with the transition was about 4 K. The DSC traces for the other compounds were measured during heating but not cooling so there is no information about any hysteresis associated with those transitions, but endotherms, which point to first-order transitions, were observed for all compounds with two-dimensional hydrogen bonding.

A first-order transition should have a measurable ΔV, but that value is not easily measured in the absence of determination of the cell constants as a function of T. The temperature gap between the cell constants determined for the higher- and lower-temperature phases was in the range 17–29 K, so that we could be sure that the transition was complete. The volumes per formula unit (V/Z) for the two phases are therefore not really comparable. The greatest change was for M = Mn, $Z' = 3$ (267 K) $\rightarrow$ $Z' = 2$ (294 K), where V/Z increased by 3.2 Å^3 (Hao, Siegler *et al.*, 2005). Mostly, however, the changes were so small as to be insignificant relative to their estimated errors.

The transition for the M = Co compound (three-dimensional hydrogen-bond pattern) would be the most likely to be suspected of being second order because it is an order–disorder transition; it is, however, also associated with the largest ΔV: +3.4 Å^3 (0.8%) between 294 and 323 K. The transition must be first order since its ΔH is clearly non-zero.

4.2. Directions of important interionic interactions

Examination of space-filling models using the program *MERCURY* (Macrae *et al.*, 2006) shows that the crown ligands are in close contact along **a** (the horizontal direction in the top drawing of Fig. 1), the direction along which there is perfect alternation of conformational enantiomers. The crown ligands are also in contact along **c**, along which the alternation pattern varies. The crown ligands are not quite in contact along **b** (vertical axis in Fig. 1), and they are well separated along all other combinations of **a**, **b** and **c**. If the modulations are a consequence of contacts between crown ligands (see Hao, Siegler *et al.*, 2005) then the important directions are **a** and **c**. Along **a** the enantiomeric alternation is perfect because the contacts would be impossibly short if it were not; the origin of the modulations must therefore be sought along the **c** direction. We suggested a rationale for the modulations (Hao, Siegler *et al.*, 2005) based on the conflict between close packing of crown ligands, which would result in uneven spacing of metal ions, and an even spacing of metal ions, which would lead to a more regular pattern of hydrogen bonds between the axial water ligands and the nitrate counterions.

4.3. Superspace description?

If the two conformational enantiomers of the cation are colored differently, and if a packing diagram of the cations in a single layer perpendicular to **b** is drawn (see Fig. 9) then a pattern is easily seen. Along the directions $\mathbf{a}_{\frac{1}{2}} \pm \mathbf{c}_{\frac{1}{2}}$ (where the subscript refers to the Z' value, which is here that of the $Z' = \frac{1}{2}$ subcell) groups of Z' homochiral cations alternate. So in the structures with $Z' = 3$ the pattern along $[1\ 0\ \pm1]_{\frac{1}{2}} = [3\ 0\ \pm2]_3 = [1\ 0\ \pm2/3]_3$ is ... *R R R S S S R R R S S S* ..., where *R* and *S* distinguish the two conformational enantiomers. In the Cu structure with $Z' = 5$ the pattern along $[1\ 0\ \pm1]_{\frac{1}{2}} = [5\ 0\ \pm2]_5 = [1\ 0\ \pm2/5]_5$ is ... *R R R R R S S S S S R R R R R S S S S S* .... In the structures with $Z' = 8$ the pattern along $[1\ 0\ \pm1]_{\frac{1}{2}} = [8\ 0\ \pm2]_8 = [4\ 0\ \pm1]_8$ is made even more complicated by the disorder: ... *R R R R*/*S S S S S*/*R R R R R*/*S S S S S*/*R* ..., although the maximum value of the smaller occupancy factor is never much larger than 0.25.

Because patterns in which units are the same are usually easier to identify than patterns in which two units alternate, the pattern along $[1\ 0\ \pm1]_{\frac{1}{2}}$ may be seen as a stair-step pattern in which there is a step after every Z' cations. This pattern was identified for the Cu $Z' = 5$ phase by Schoenleber & Chapuis (2004; see their Fig. 2), who did a superspace refinement of that structure. While identification of this pattern may have facilitated their refinement, we note that the pattern is a consequence of the absolute alternation of conformational enantiomers along **a** and imperfect alternation along **c**. Because $\mathbf{a}_{Z'}$ and $\mathbf{c}_{Z'}$ are the directions in which the cations are actually in contact we believe it is more informative to focus on the patterns along $\mathbf{a}_{Z'}$ and $\mathbf{c}_{Z'}$ than along $[1\ 0\ \pm1]_{\frac{1}{2}}$. There are no direct cation–cation interactions along the $[1\ 0\ \pm1]_{\frac{1}{2}}$ directions.

In the reconstructed reciprocal-lattice slices the superstructure reflections appear to the eye to be densest along lines parallel to $\mathbf{c}^*_{Z'}$, but are stronger if h is odd than if h is even. In the case of the $Z' = 5$ structure (M = Cu) the strongest reflections, which correspond to the subcell (or basic cell), have h even and $\ell = 5n$. The second strongest set of reflections has h odd and $\ell = 5n \pm 2$, which explains the choice of $q = (\frac{1}{2}, 0, -\frac{2}{5})$ by Schoenleber & Chapuis (2004).

In the $Z' = 3$ structures the strongest set of reflections has h even and $\ell = 3n$. The second strongest group has h odd and $\ell = 3n \pm 1$. In the $Z' = 8$ structure the strongest reflections again have h even and $\ell = Z'n$, and the second strongest set has h odd and $\ell = 8n \pm 3$ (see Figs. 4 and 5). (In the $B2_1$ cell used for the $Z' = 8$ structure the parity of the h and ℓ indices must be the same so the reflections with h even and ℓ odd, or *vice versa*, have $I = 0$.)

Simulations show that the intensity patterns for the $\ell = Z'n \pm m$ reflections are those expected for a row of two kinds of equally spaced points that alternate in the ways seen for the $Z' = 2$, 3, 5 and 8 phases if the two kinds of points have similar scattering powers. The actual intensities of the $\ell = Z'n \pm m$, $m \neq 0$, reflections, however, are much greater than they are in the simulations because the cations in the actual structures are not quite equally spaced.

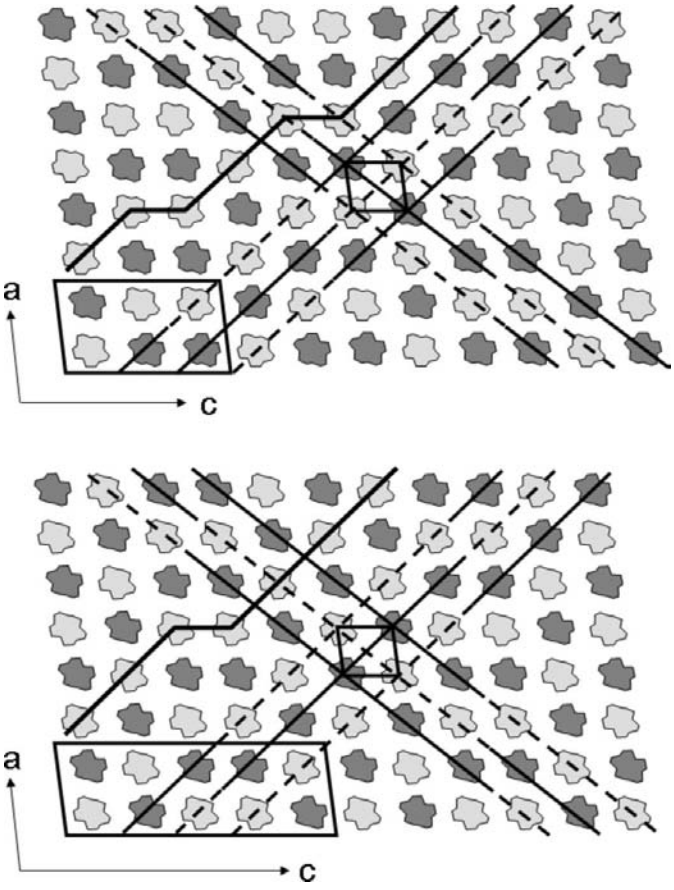

Figure 9
Alternation patterns in the ***ac*** planes (*e.g.* $y = 0$) for the structures with $Z' = 3$ (upper drawing) and $Z' = 5$ (lower drawing). In each case one of the two sets of conformational enantiomers has been darkened so that the alternation patterns can be seen. The unit cell is shown in the lower left of each drawing; the basic cell (or subcell) is shown in the middle of each drawing. The alternation parallel to **a** is strict; the alternation parallel to **c** fails once in every Z' pairs. This pattern leads to a stair-step pattern of homochiral conformers that is shown by a heavy line in the upper-left of each drawing. It also leads to lines along [1 0 ±1] of the basic cell along which Z' cations of one conformational enantiomer (solid line segments) alternate with Z' cations of the other conformational enantiomer (dashed line segments). Drawings for the $Z' = 2$ and $Z' = 8$ modulated variants are analogous.

4.4. Choice between a conventional and a superspace refinement

Initially we chose to do conventional refinements using *SHELXL*97 (Sheldrick, 2008) because that was the software with which we were familiar. We encountered no difficulties with this approach and so saw no need to do a superspace refinement. We did, however, have to impose geometrical restraints in the case of the room-temperature $Z' = 8$ structures to keep the distances and angles similar. Constraints to keep the displacement parameters for the Z' formula units had to be imposed at room temperature or above if Z' was ≥ 5.

Conventional refinements were successful because most of the supercell reflections had intensities large enough that they could be measured accurately, especially with radiation from a focused rotating-anode source.

4.5. Final note

After this study was essentially complete Dr Rob Hooft of Bruker AXS Delft integrated the original frames measured with a KappaCCD diffractometer for the $Z' = 8$ phase of the M = Fe compound at 90 K (Hao, Siegler *et al.*, 2005) using the software package *EvalCCD* (Duisenberg *et al.*, 2003), which allows for incommensurate modulations. He found a basic unit cell that is related by the matrix $(\frac{1}{2}00/010/00\frac{1}{8})$ to the $B2_1$ cell reported here; the modulation vector associated with this basic cell is q = (0.500, 0.000, −0.380) with uncertainties in the vector components of less than 0.001. The vector q is then $[\frac{1}{2}, 0, -\frac{3}{8}–0.005\ (1)]$. The reflections from the basic cell account for 64% of all intensity, and the first-order satellites for an additional 27%; the intensities of the second- and third-order satellites (5 and 4%) are comparable. The modulation vector referred to the $B2_1$ cell is (1, 0, −3.04), which is perpendicular to the direct-space vector [3.04, 0, 1] and essentially parallel to $[1.02, 0, -\frac{1}{8}]$.

The structure is at least almost commensurate. In any event we do not find that the modulation vector helps us better understand the structure or the reconstructed $hn\ell$ slices of the diffraction pattern.

5. Summary

A second phase has been found for each of five $[M(H_2O)_2$(15-crown-5)$](NO_3)_2$ compounds, M = Mg, Co, Ni, Cu, Zn. Two phases for the Fe compound and three for the Mn compound were already known (Hao, Siegler *et al.*, 2005).

Six of the seven compounds (*i.e.* all except M = Co) have structures with a two-dimensional hydrogen-bonding pattern. Each of these compounds has two phases between 275 and 306 K that are linked by a reversible transition during which crystallinity is preserved. The transitions are probably first-order.

All phases with two-dimensional hydrogen-bonding patterns can be viewed as modulated variants of a disordered

$P2_1/c$, $Z' = \frac{1}{2}$ structure in which the $[M(H_2O)_2$(15-crown-5)] cation would lie on an inversion center. In all structures actually observed there is perfect alternation of conformationally enantiomeric cations along a doubled **a** axis of this basic cell. There is also alternation of conformational enantiomers along **c** of this basic cell, with the length of **c** being multiplied by Z'.

(i) $Z' = 3$: Every third pair of cations along **c** is conformationally homochiral.

(ii) $Z' = 8$: Every fourth pair of cations along **c** is conformationally homochiral.

(iii) $Z' = 5$: Every fifth pair of cations along **c** is conformationally homochiral.

(iv) $Z' = 2$: Alternation of conformationally enantiomeric cations is perfect.

Three types of transitions have been found (the Z' value for the phase stable at the lower temperatures is given first):

(i) Z' 3 $\leftrightarrow$ 8 (Mg, Fe, Zn) (or 1 alternation failure in three contacts $\leftrightarrow$ 1 in 4),

(ii) Z' 3 $\leftrightarrow$ 2 (Mn, Ni) (or 1 alternation failure in 3 contacts $\leftrightarrow$ none), and

(iii) Z' 5 $\leftrightarrow$ 2 (Cu) (or 1 in alternation failure in 5 contacts $\leftrightarrow$ none).

In all cases the higher-temperature phase has more perfect alternation of enantiomers than does the lower-temperature phase. There is minor disorder at two sites in the $Z' = 8$ structures, but not in any of the others.

The reasons for the variability of the modulation patterns are not yet understood.

We have not isolated the basic, disordered $P2_1/c$, $Z' = \frac{1}{2}$ structure that we thought might be found above room temperature for at least one of the metal ions.

For M = Co the two phases have a three-dimensional hydrogen-bonding pattern and the transition is of the order-disorder type ($P4_1$, $Z' = 2 \leftrightarrow P4_12_12$, $Z' = \frac{1}{2}$). A very similar ordered $P4_1$ phase has also been found for M = Mn (Hao, Siegler *et al.*, 2005), but any transition to a disordered phase takes place at a higher temperature than we could reach.

The unusually rich phase behavior in this system occurs because the atomic displacements necessary to interconvert conformationally enantiomeric cations are small. The activation energy for the interconversion is also small. The changes do, however, lead to an overall change in cation shape large enough to affect the crystal packing.

M. A. Siegler thanks the University of Kentucky for a 2006–2007 Kentucky Opportunity Fellowship. We thank Professor Mark D. Watson of the University of Kentucky Chemistry Department for help with the DSC measurements. We are very grateful to Dr Rob Hooft of Bruker AXS Delft for determining how much the M = Fe structure might deviate from being commensurately modulated. We are grateful to the National Science Foundation (MRI No. 0319176) for funds to purchase the Bruker–Nonius X8 Proteum diffractometer.

References

Bruker–Nonius (2004). *APEX*2. Bruker-Nonius AXS Inc., Madison, Wisconsin, USA.
Duisenberg, A. J. M., Kroon-Batenburg, L. M. J. & Schreurs, A. M. M. (2003). *J. Appl. Cryst.* **36**, 220–229.
Flack, H. D. (1983). *Acta Cryst.* A**39**, 876–881.
Greenwood, N. N. & Earnshaw, A. (1997). *Chemistry of the Elements*, 2nd ed. Oxford: Butterworth-Heinemann.
Hao, X. (2005). PhD Dissertation. University of Kentucky, USA.
Hao, X., Parkin, S. & Brock, C. P. (2005). *Acta Cryst.* B**61**, 675–688.
Hao, X., Siegler, M. A., Parkin, S. & Brock, C. P. (2005). *Cryst. Growth Des.* **5**, 2225–2232.
Herbstein, F. H. (2000). *Acta Cryst.* B**56**, 547–557.
Holt, E. M., Alcock, N. W., Hendrixson, R. R., Malpass, G. D., Ghirardelli, R. G. & Palmer, R. A. (1981). *Acta Cryst.* B**37**, 1080–1085.
Macrae, C. F., Edgington, P. R., McCabe, P., Pidcock, E., Shields, G. P., Taylor, R., Towler, M. & van de Streek, J. (2006). *J. Appl. Cryst.* **39**, 453–457.
Nonius (1999). *COLLECT*. Nonius BV, Delft, The Netherlands.
Otwinowski, Z. & Minor, W. (2006). *International Tables for Crystallography*, Vol. F., ch. 11.4, pp. 226–235.
Rogers, R. D. & Song, Y. (1995). *J. Coord. Chem.* **34**, 149–157.
Schoenleber, A. & Chapuis, G. (2004). *Ferroelectrics*, **305**, 99–102.
Sheldrick, G. M. (2008). *Acta Cryst.* A**64**, 112–122.
Siegler, M. A. (2007). PhD Dissertation. University of Kentucky.
Siegler, M. A., Parkin, S., Selegue, J. P. & Brock, C. P. (2008). *Acta Cryst.* B**64**, 725–749.
Xia, A., Selegue, J. P., Carrillo, A., Patrick, B. O., Parkin, S. & Brock, C. P. (2001). *Acta Cryst.* B**57**, 507–516.
Xia, A., Selegue, J. P., Carrillo, A., Patrick, B. O., Parkin, S. & Brock, C. P. (2002). *Acta Cryst.* B**58**, 565.